



Bizarre dermal armour suggests the first African ankylosaur

Susannah C. R. Maidment^{1,2}✉, Sarah J. Strachan³, Driss Ouarhache⁴, Torsten M. Scheyer⁵, Emily E. Brown^{1,2}, Vincent Fernandez¹, Zerina Johanson¹, Thomas J. Raven^{1,6} and Paul M. Barrett^{1,7}

Ankylosauria is a diverse clade of armoured dinosaurs whose members were important constituents of many Cretaceous faunas. Phylogenetic analyses imply that the clade diverged from its sister taxon, Stegosauria, during the late Early Jurassic, but the fossil records of both clades are sparse until the Late Jurassic (~150 million years ago). Moreover, Ankylosauria is almost entirely restricted to former Laurasian continents, with only a single valid Gondwanan taxon. *Spicomellus afer* gen. et sp. nov. appears to represent the earliest-known ankylosaur and the first to be named from Africa, from the Middle Jurassic (Bathonian-Callovian) of Morocco, filling an important gap in dinosaur evolution. The specimen consists of a rib with spiked dermal armour fused to its dorsal surface, an unprecedented morphology among extinct and extant vertebrates. The specimen reveals an unrealized morphological diversity of armoured dinosaurs during their early evolution, and implies the presence of an important but undiscovered Gondwanan fossil record.

Ankylosauria is a diverse clade of armoured herbivorous dinosaurs characterized by the possession of a diversity of osteoderms located on the skull, dorsal surface of the body and tail^{1,2}. Ankylosaurs diverged from their sister-taxon, Stegosauria, in the late Early or early Middle Jurassic, but their fossil record at this time is extremely sparse^{2–4}. Indeed, the only valid Middle Jurassic ankylosaur is *Sarcolestes leedsi*, represented by a partial lower jaw⁵. Ankylosauria increased in diversity in the Early Cretaceous, becoming important constituents of Late Cretaceous ecosystems, and went extinct along with other non-avian dinosaurs at the end-Cretaceous mass extinction^{1–4}. Ankylosaurs are well-known on the former Laurasian continents, but their fossil record in Gondwana is highly fragmentary with only a single valid taxon being recognized⁶, although tantalizing fragmentary material suggests that they were more widespread. Here we describe a new specimen that we interpret as an ankylosaur from the Middle Jurassic (Bathonian/Callovian) of the Middle Atlas Mountains of Morocco – the first from Africa. The specimen fills a gap in the fossil record of Ankylosauria, suggesting that shortly after their evolution, ankylosaurs had attained a global distribution, and indicates an important but as yet undiscovered armoured dinosaur fossil record in the Jurassic of Gondwana.

Results

Dinosauria Owen, 1842⁷

Ornithischia Seeley, 1887⁸

Ankylosauria Osborn, 1923⁹

Spicomellus afer gen. et sp. nov.

LSID: urn:lsid:zoobank.org:act:D12DDAB4-E164-411D-8406-B7B3DEC52F71

Etymology. *Spicus* meaning spike (Latin); *mellus*, a collar with spikes (Latin). A reference to the morphology of the specimen. *Afer* (Latin), an inhabitant of Africa.

Holotype. NHMUK PV R37412, a partial rib bearing four co-ossified spines (Fig. 1a–d) housed at the Natural History Museum, London (NHMUK).

Horizon and locality. El Mers III Formation (Upper Bathonian/Callovian, Middle Jurassic: 168.3–163.5 million years ago), Boulahfa, south of Boulemane, Fez-Meknes, Morocco (detailed locality information can be found in ref. ⁴). Maidment et al.⁴ reported the horizon as lying in the El Mers II Formation, but subsequent field observations at the site suggest that it may lie slightly higher in the stratigraphy.

Diagnosis. Differs from all other armoured dinosaurs in possessing ‘T’-shaped dorsal ribs with a fused, rod-like osteoderm on the dorsal surface, from which projects a series of co-ossified conical dermal spines.

Osteological description. NHMUK PV R37412 is a slightly curved dorsal rib fragment fused to a flat plate-like osteoderm and bearing four elongate, conical spines that project from its dorsal surface (Fig. 1a–d). The specimen was scanned using X-ray Computed Tomography (XCT) to confirm that the spines are co-ossified (Fig. 1c,d, Extended Data Figs. 1–3 and Supplementary video). In cross-section, the rod is strongly ‘T’-shaped, with its dorsal, horizontally oriented flange being broader anteroposteriorly (58 mm maximum width) than the depth of its ventral flange (33 mm maximum depth). The dorsal surface of the horizontal flange bears clear fibres that extend along the surface parallel to the rod’s long axis, as well as several fainter fibres extending perpendicular to the clear fibres. The dorsal, anterior and posterior surfaces of the rod are rugose. The horizontal and vertical flanges merge via a concave, smooth surface. The change in texture from the dorsal, rugose horizontal bar to the smooth, featureless ventral flange is marked by a groove that extends for the entire length of the rod.

¹Department of Earth Sciences, Natural History Museum, London, UK. ²School of Geography, Earth and Environmental Sciences, University of Birmingham, Birmingham, UK. ³Department of Earth Sciences, University College London, London, UK. ⁴GERA Laboratory, Faculty of Sciences Dhar El Mahraz, SMBA University, Fez, Morocco. ⁵Palaeontological Institute and Museum, University of Zurich, Zurich, Switzerland. ⁶School of Environment and Technology, University of Brighton, Brighton, UK. ⁷Evolutionary Studies Institute, University of the Witwatersrand, Johannesburg, South Africa. ✉e-mail: susannah.maidment@nhm.ac.uk

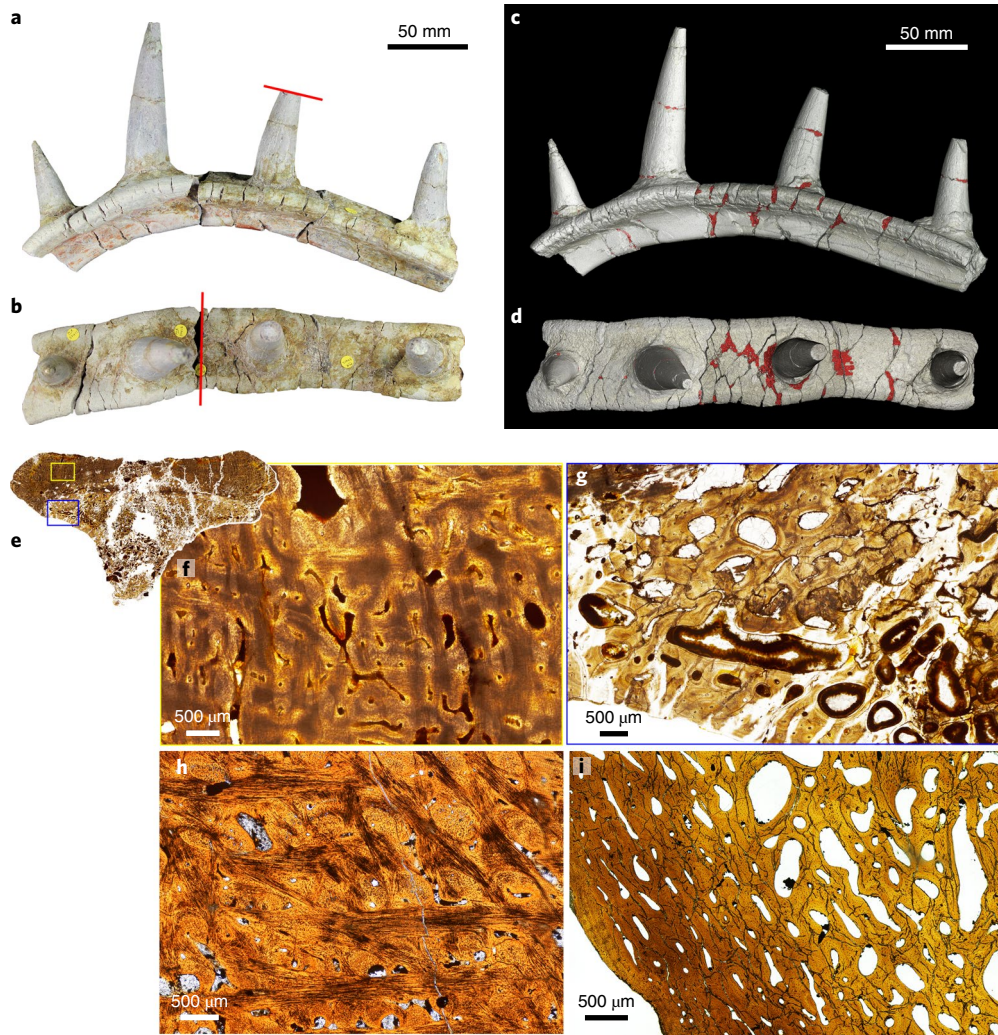


Fig. 1 | Morphology and histology of *Spicomellus afer*, NHMUK PV R37412. **a–d**, Photographs (**a,b**) and 3D model produced from XCT scanning (**c,d**) showing the specimen in anterior/posterior (**a,c**) and dorsal (**b,d**) views. Red lines on **a** and **b** indicate where the specimen was sectioned for histological analysis. Red colouration on **c** and **d** indicates a cement used to consolidate the specimen. **e–g**, Thin-section photographs of the rod: full section of the rod (**e**) (see Fig. 2a for larger version); histological section through the dorsal osteodermal part of the rod (**f**) showing structural fibre bundles in an orthogonal 'plywood-like' arrangement; histological section through the rib part of the rod (**g**) showing heavily remodelled cortical bone. Yellow box in **e** indicates the position of **f**, blue box indicates the position of **g**. **h**, Histological section from the sacral shield of NHMUK PV R9293, an indeterminate ankylosaur from the Lower Cretaceous Wealden Group of the UK showing fibre bundles arranged in a pattern similar to that of the osteoderm in *Spicomellus* (**f**). **i**, Histological section from the rib of NHMUK PV R36643, an unnamed ankylosaur from the Callovian Oxford Clay Formation of the UK showing well-vascularized, remodelled cortical bone similar to that of the rib section of *Spicomellus* (**g**).

The spines are rounded in cross-section and project dorsally (Fig. 1a–d). The medialmost spine is the smallest and is complete (54 mm from base to tip). As preserved, the second spine is the tallest (97 mm, but missing its distal tip), and the third spine is broken. The fourth spine is angled slightly medially, although this is probably taphonomic distortion (55 mm long, missing its distal tip). The surfaces of the spines are generally smooth, but there is a fine anastomosing mesh of vascular imprints on the external surface.

Histological description. The spine (Fig. 2b and Extended Data Fig. 4) consists of a ~2.5 mm thick symmetrical cortex of woven bone and an inner core of highly vascularized trabecular bone. Several long pipes¹⁰ extend from the core, opening on the surface. A thin layer, which is translucent in plane-polarized light and birefringent under crossed polars, covers much of the outer surface; it includes many scattered small osteocyte lacunae, and is probably diagenetic. Radial vascular canals also open to the bone surface. At

least nine growth lines, visible as thin, dark, undulating lines parallel to the bone surface, extend from the central region of the cortex, becoming more closely spaced towards the outer surface. The woven bone matrix of the cortex is dominated by primary osteons with occasional radial and reticular vascular canals in circumferential arrangement. Scattered secondary osteons are present from the inner core to the mid-cortex. The core is composed of trabecular bone and large resorption cavities lined with lamellar bone and occasional secondary osteons. Many small, irregularly arranged osteocyte lacunae with small or no visible processes are scattered throughout the primary bone. Osteocyte lacunae in remodelled bone have a slightly more ovate shape and more extensive processes.

The horizontal bar of the rod is composed of two distinct histologies (Figs. 1e–g and 2a,c). Its upper and lower sections are divided by a strip of structural fibres (mineralized collagenous fibres not associated with ligamentous or tendinous insertion¹¹) that extend across the width of the section (Figs. 1e and 2a,c). The upper half

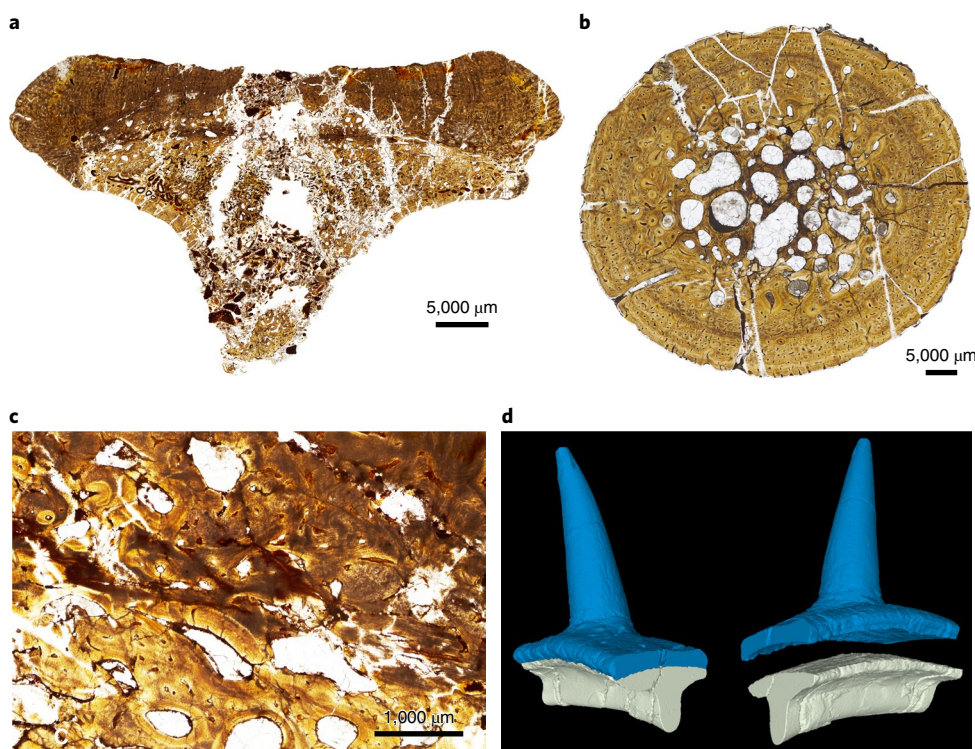


Fig. 2 | Details of the histology of *Spicomellus afer*, NHMUK PV R37142. a, c, Thin-section photographs of the fused rib and osteoderm. The darker region at the top of the image in **a** and to the top left of the image in **c** bears the histological characteristics of an osteoderm, while the lighter region below bears histological characteristics of the rib. A strip of structural fibres extending across this interface can be observed in **c**. **b,** Thin-section photograph of the spine of NHMUK PV R37142 *S. afer* showing a cortex of woven bone and an inner core of highly vascularized trabecular bone. **d,** A section of NHMUK PV R37142 *S. afer* with the osteoderm and rib sections segmented separately so the morphology of each can be seen. The osteoderm is in blue, while the rib is shown in white.

of the rod is dominated by an ordered pattern of structural fibres, which are arranged in regular, orthogonal plywood-like layers¹² that cross each other at approximately 90° and overlie the primary bone matrix. The fibres, visible as darker and lighter strands or bundles under polarized light (Fig. 1f and Extended Data Fig. 5), are arranged approximately perpendicular and parallel to the bone surface and follow the curvature of the bone at its outer edges (Fig. 2a). The fibre bundles are 500–600 μm thick and the majority are not interwoven. Simple vascular canals and some primary osteons with occasional radial and reticular vascular canals can be seen in the small sections of primary bone matrix that are not obscured by the fibre bundles (Fig. 1f). Small, irregular osteocyte lacunae with short or no visible processes are present.

By contrast, the lower section of the horizontal bar and the vertical flange are composed of highly vascularized, remodelled woven bone with no structural fibres (Figs. 1g and 2a). Growth lines are visible near the outer surface. Small, simple vascular canals are present in a circumferential arrangement parallel to the outer surface, followed by a ring of larger primary osteons and then either a sharp transition or smooth gradation to a highly vascularized region populated by resorption cavities with lamellar bone infill forming trabeculae with a high degree of remodelling (Figs. 1g and 2a). At least three generations of secondary osteons are present (Fig. 1g). Many small osteocyte lacunae are present with short or no visible processes, whereas the osteocyte lacunae in remodelled bone are more ovate with more extensive processes.

Taxonomic identity. Given its unique anatomy, we considered a non-tetrapod osteichthyan affinity for NHMUK PV R37412, but rejected this hypothesis for several reasons. First, the specimen

was found in a terrestrial sedimentary sequence⁴, which seems an unlikely source for what would have been an exceptionally large fish, but exclusion is also possible based on histological criteria. Teeth are ankylosed to the jaw in a range of osteichthyan fishes¹³, similar to the way the spikes are fused to the rod in NHMUK PV R37412. However, fish teeth are usually composed of orthodontine surrounding a pulp cavity, with characteristic elongate odontoblast tubules extending through the dentine¹³. Several chondrichthyans^{14–16} and a few osteichthyans¹³ have trabecular bone-like osteodentine within the pulp cavity, but in the latter this is generally surrounded by a pallial layer of orthodontine. However, there is no histological evidence of orthodontine in the specimen and other aspects of its histology and morphology favour a tetrapod origin.

Osteoderms are thought to form via metaplasia, a specific case of intramembranous ossification^{11,17,18} but see¹⁹. Metaplastic bone typically has low levels of vascularity and small or no osteocyte lacunae that lack visible processes^{17,18}. Bone formed via metaplasia from the dermis often exhibits extensive fibre patterns reflecting the incorporation of collagen fibres from the original extracellular matrix^{11,18,20}. The presence of extensive structural fibre bundles in the upper part of the horizontal bar strongly suggests that it is an osteoderm formed via intramembranous ossification within the stratum compactum, and indicates that the skin would have been reinforced with thick striations of structural fibres, adding strength and tear resistance²¹. The lower part of the rod bears the histological characteristics of tetrapod postcranial bone²², and is morphologically consistent with being a dorsal rib.

Consequently, we conclude that NHMUK PV R37412 is a dorsal rib with an osteoderm fused to its external surface (Fig. 2d). The morphological and histological characteristics of NHMUK

PV R37412, along with its age, suggest referral to Ankylosauria. Possession of dorsal ribs that are ‘T’-shaped in cross-section in their proximal portions is a synapomorphy of Eurypoda (Stegosauria + Ankylosauria)^{1,23}, allowing confident referral to the clade. Among eurypodans, the interwoven, plywood-like arrangement of structural fibres observed in this specimen has previously been described in numerous ankylosaurs^{11,24,25} (Fig. 1h); in contrast, in stegosaurs, only the osteoderms of *Stegosaurus* have been histologically investigated, and while these possess mineralized fibres around their bases¹⁰, they do not have a plywood-like arrangement¹¹. Mineralized fibre bundles have been observed in the early-diverging armoured dinosaur *Scelidosaurus* (which is either the sister taxon to Eurypoda⁴ or to Ankylosauria²⁶), but these do not have a plywood-like arrangement either^{11,24}. It has been suggested that the osteoderms of *Scelidosaurus* represent the plesiomorphic condition for Ankylosauria¹¹, and that the unique possession of a plywood-like arrangement of structural fibres in the osteoderms of ankylosaurs indicates an increased contribution from the dense connective tissues of the stratum compactum during osteoderm skeletogenesis relative to that of other thyreophorans²⁵. It is therefore most parsimonious to consider that the plywood-like arrangement of structural fibre bundles is a synapomorphy of Ankylosauria within Thyreophora based on the evidence currently available, a conclusion also reached by other authors^{11,25}. The plywood-like arrangement of structural fibres therefore supports referral of *S. afer* to Ankylosauria^{11,18,24,25}.

This structural fibre arrangement is also known in other tetrapods, including turtles^{24,27}, aetosaurs²⁸, phytosaurs^{29,30}, and titanosaurian sauropods³¹, but NHMUK PV R37412 can be excluded from referral to any of these groups on morphological and stratigraphic grounds. No known phytosaur osteoderms are spine-like³², but those of some aetosaurs are³³. However, both phytosaurs and aetosaurs went extinct before the end of the Triassic^{30,33}, so referral to these groups would invoke an unprecedented 30–40 million-year ghost lineage in either case. A few turtles possess osteoderms²⁴, including conical spines³⁴, but their osteoderms are much smaller than those of NHMUK PV R37412 and often have a characteristic pustulate surface texture. Titanosaurid sauropods lack spine-like osteoderms^{29,31} and the clade did not originate until the Cretaceous³⁵, requiring a 23 million-year ghost lineage. By contrast, the armoured dinosaurs possessed a wide variety of plate- and spine-like osteoderms and originated in the Early Jurassic^{2,4}.

Discussion

The identification of NHMUK PV R37412 as an ankylosaur dorsal rib with fused osteoderms indicates that it was located on the trunk with its spines extending laterally. This armour morphology is unlike that of any other thyreophoran. Stegosaurs possess spines in the caudal region, but these oriented parasagittally, are greatly hypertrophied, and are oval rather than round in cross-section³⁶. Ankylosaurs possess a wide variety of dermal armour morphologies generally arranged in transverse rows across the neck and trunk²⁵, in an arrangement similar to that seen in *Spicomellus*. However, no known ankylosaur possesses conical spines fused to rod-like osteoderms, which in turn are fused to external rib surfaces. Indeed, to our knowledge, no other vertebrate, extant or extinct, possesses osteoderms directly fused to the dorsal ribs (turtle carapace elements are not modified osteoderms²⁷). Ornamented ribs are known in the Triassic cynodont *Protuberum cabralensis*³⁷ and the Triassic pseudosuchian *Euscolosuchus olseni*³⁸, but in neither of these taxa is the ornamentation dermal in origin^{37,38}. *Spicomellus* suggests that early ankylosaurs displayed unrealized morphological diversity and experimented with the skeletal developmental processes underpinning the origin of these features. We speculate that the ‘T’-shaped cross-section of this armoured rod exploited its wide upper section to spread applied loads and to increase its ability to resist

compression, while its vertical flange reduced internal bending moments and resisted buckling. Hence, this fused structure might afford greater protection in the event of a predator attack than isolated spikes alone.

The oldest stegosaur, *Isaberrysaura*, is Bajocian in age³⁹ and indicates that Stegosauria and Ankylosauria had already diverged by the early Middle Jurassic. *Sarcolestes leedsi* is the only other named Middle Jurassic ankylosaur, represented by a partial lower jaw from the Callovian Oxford Clay Formation of the UK⁵. *Spicomellus* therefore represents the oldest ankylosaur identified so far. Ankylosaurs have a predominantly Laurasian distribution, where they were important components of Late Cretaceous ecosystems¹. Only a single valid species, *Kunbarrasaurus ieveri*, is currently known from Gondwana⁶, although indeterminate remains have also been described^{3,40–47}. African ankylosaur remains are unknown, however. The presence of *Spicomellus* in the Bathonian of northern Africa indicates that Ankylosauria had a near-global distribution by the Middle Jurassic. This suggests an important hidden radiation of Early–Middle Jurassic thyreophorans, which must have occurred shortly after the first appearance of ornithischians in the fossil record.

Stegosaurs appear to have gone extinct in the Early Cretaceous, at the same time that ankylosaurs increased in diversity, leading to suggestions that ankylosaurs outcompeted stegosaurs⁴. However, both clades co-occurred in Jurassic ecosystems: *Spicomellus* and *Adratiklit* in the Middle Jurassic El Mers III Formation⁴; *Sarcolestes*⁵ and *Loricatosaurus*³⁶ in the Middle Jurassic Oxford Clay Formation; *Gargoyleosaurus*⁴⁸, *Mymoorapelta*⁴⁹, *Stegosaurus*³⁶, *Hesperosaurus*⁵⁰ and *Alcovasaurus*⁵¹ in the Upper Jurassic Morrison Formation; and *Stegosaurus*, *Miragaia* and *Dracopelta* in the Upper Jurassic Lourinhã Formation⁵². This indicates long-term ecological overlap between stegosaurs and ankylosaurs for >20 million years, suggesting that the decline of stegosaurs may have been for reasons other than competition with ankylosaurs.

Methods

Acquisition of the specimen. NHMUK PV R37412 was acquired by the Natural History Museum from a commercial fossil dealer, Moussa Direct, based in Cambridge, UK. The locality information was provided by Moussa Direct and confirmed through discussion with the Moroccan fossil dealer who sold it to Moussa Direct. S.C.R.M. and D.O. visited the locality in 2019 and 2020, respectively, to study the sedimentology and stratigraphy, and the results of these investigations are reported in Maidment et al.⁴ and herein. Work on this specimen was conducted via a Memorandum of Understanding between the UK Natural History Museum and the Université Sidi Mohamed Ben Abdellah, Morocco.

XCT. The specimen was characterized with a Nikon HMX ST 225 CT system (Nikon Metrology) using XCT. The four parts of the specimen were scanned together, ensuring identical characterization from XCT. The instrument was set up to obtain an appropriate transmission of X-rays through the sample. The experimental conditions consisted of a Nikon Ultrafocus X-ray source with a static Tungsten target; voltage of 215 kV and current of 232 μ A (power of 49.88 W); filtration with 1 mm silver; detector digital gain set to 12 dB. The acquisition consisted of 3,142 projections of 1.415 s each with a frame averaging of 2. The magnification from the X-ray conical beam generated data with a voxel size of 89.428 μ m. The tomographic reconstruction was performed using Nikon CT-agent software (Nikon Metrology). The centre of rotation was calculated on two slices (located 25% from the top and the bottom of the volume, respectively). Before reconstruction, we used the automated beamhardening correction option, manually thresholding the specimen from the surrounding background. The tomographic reconstruction was first done at a 32-bit volume and later converted to a 16-bit uncompressed raw volume using percentiles of 0.01% and 99.99% to convert the 32-bit histogram.

Reconstruction and analysis. Reconstruction of the specimen (Fig. 1c,d) was completed using VG Studio MAX 3.2 (Volume Graphics). Each part of the specimen was segmented and extracted to be manipulated individually. Alignment of each individual part was done manually, verifying the continuity of features on both the external surfaces and between slices. Once two parts were considered properly aligned, their positions were locked and a new part was added and aligned.

Assessment of specimen authenticity. The CT data were carefully examined to determine if the fossil had been altered. First, we looked for material that was not

the infilling matrix or the fossilized bone. A grainy material is present in several parts of the specimen, located in cracks (Extended Data Fig. 1 and Supplementary video). It is very likely that this represents a type of cement that was used to consolidate the material and attach parts that were broken. For instance, most of the spikes are broken at their base and have been attached with this material. It is clear to see on the CT data that the modification of the specimen consisted solely of re-attaching these broken parts. Features in the trabecular and the cortical bone show clear continuity on both sides of these cracks (Extended Data Fig. 2). Finally, the presence of a continuous cortical layer surrounding the entire specimen (with the exceptions of the two fractured ends) indicates that the specimen was not modified by carving.

Segmentation. Once histological analysis had determined that the upper part of the rod and spikes was osteodermal while the lower part was a rib, the CT data were inspected so that the osteoderm and rib could be segmented out. This was carried out on one section of the specimen (Fig. 2d and Extended Data Fig. 3a). First, sections of the specimen were examined in CT data (Extended Data Fig. 3b(1–5)) and the boundary between osteodermal and cortical bone identified (Extended Data Fig. 3c). The parts were then labelled (Extended Data Fig. 3d) and segmented separately (Fig. 2d) to show the morphology of the osteoderm and the rib.

Histological Analyses. Thin sections were prepared in accordance with standard histological practices for fossil bone^{53,54} and examined under a polarizing microscope. To determine whether the rod was likely positioned internally or externally (including within the dermis and thus if it could be considered an osteoderm), the histology was compared to thin sections and descriptions of thyreophoran osteoderms and ribs^{55–57} (Fig. 1h,i), which were considered to be the most likely internal bone that could have formed the lower part of this structure. The rod was sectioned transversely and two horizontal sections were cut from one spine. Slides were cut to a thickness of $80\pm 5\ \mu\text{m}$ and examined under a Brunel (SP250P) polarizing microscope using plane- and cross-polarized light, with the addition of a lambda waveplate. Macro-images of the slides were taken using an Axio Imager M2 with an AxioCam HR RS camera. Basic white balance, thresholding, cropping and scaling of images were carried out using FIJI, an ImageJ plugin, Corel PaintShop Pro 19 and Adobe Photoshop.

Reporting Summary. Further information on research design is available in the Nature Research Reporting Summary linked to this article.

Data availability

All data associated with this paper are included in Extended Data. The specimen described in this study is deposited in the collections of the Natural History Museum, London, under specimen number NHMUK PV R37412. This published work and the nomenclatural acts it contains are registered with ZooBank (LSID: urn:lsid:zoobank.org:act:D12DDAB4-E164-411D-8406-B7B3DEC52F71LSID: urn:lsid:zoobank.org:act:D12DDAB4-E164-411D-8406-B7B3DEC52F71).

Received: 7 July 2021; Accepted: 9 August 2021;

Published online: 23 September 2021

References

- Vickaryous, M. K., Maryańska, T. & Weishampel, D. B. in *The Dinosauria* (eds Weishampel, D. B. et al.) 363–392 (Univ. California Press, 2004).
- Thompson, R. S., Parish, J. C., Maidment, S. C. R. & Barrett, P. M. Phylogeny of the ankylosaurian dinosaurs. *J. Syst. Palaeontol.* **10**, 301–312 (2012).
- Arbour, V. M. & Currie, P. J. Systematics, phylogeny and palaeobiogeography of the ankylosaurid dinosaurs. *J. Syst. Palaeontol.* **14**, 385–444 (2016).
- Maidment, S. C. R., Raven, T. J., Ouarhache, D. & Barrett, P. M. North Africa's first stegosaur: implications for Gondwanan thyreophoran dinosaur diversity. *Gondwana Res.* **77**, 82–97 (2020).
- Galton, P. M. *Sarcolestes leedsi* Lydekker, an ankylosaurian dinosaur from the Middle Jurassic of England. *Neues Jahrb. Geol. Palaeontol. Monatsh.* **1983**, 141–155 (1983).
- Leahy, L., Molnar, R. E., Carpenter, K., Witmer, L. M. & Salisbury, S. W. Cranial osteology of the ankylosaurian dinosaur formerly known as *Minmi* sp. (Ornithischia: Thyreophora) from the Lower Cretaceous Allaru Mudstone of Richmond, Queensland, Australia. *PeerJ* **3**, e1475 (2015).
- Owen, R. Report on British fossil reptiles. *Rep. Brit. Assoc. Adv. Sci.* **11**, 60–204 (1842).
- Seeley, H. G. On the classification of the fossil animals commonly named Dinosauria. *Proc. R. Soc. Lond.* **43**, 258–265 (1888).
- Osborn, H. F. Two Lower Cretaceous dinosaurs of Mongolia. *Am. Mus. Novit.* **95**, 1–10 (1923).
- de Buffrénil, V., Farlow, J. O. & de Ricqlès, A. Growth and function of *Stegosaurus* plates: evidence from bone histology. *Paleobiology* **12**, 459–473 (1986).
- Scheyer, T. M. & Sander, P. M. Histology of ankylosaur osteoderms: implications for systematics and function. *J. Vertebr. Paleontol.* **24**, 874–893 (2004).
- Scheyer, T. M., Sander, P. M., Joyce, W. G., Bohme, W. & Witzel, U. A plywood structure in the shell of fossil and living soft-shelled turtles (Trionychidae) and its evolutionary implications. *Org. Divers. Evol.* **7**, 136–144 (2007).
- Berkovitz, B. & Shellis, R. P. *The Teeth of Non-mammalian Vertebrates* (Academic Press, 2017).
- Schnetz, L., Pfaff, C. & Kriwet, J. Tooth development and histology patterns in lamniform sharks (Elasmobranchii, Lamniformes) revisited. *J. Morphol.* **277**, 1584–1598 (2016).
- Jambura, P. L. et al. Micro-computed tomography imaging reveals the development of a unique tooth mineralization pattern in mackerel sharks (Chondrichthyes, Lamniformes) in deep time. *Sci. Rep.* **9**, 9652 (2019).
- Jambura, P. L. et al. Evolutionary trajectories of tooth histology patterns in modern sharks (Chondrichthyes, Elasmobranchii). *J. Anat.* **236**, 753–771 (2020).
- Reid, R. E. H. Bone histology of the Cleveland-Lloyd dinosaurs and of dinosaurs in general, part 1: introduction to bone tissues. *BYU Geol. Stud.* **41**, 25–72 (1996).
- Main, R. P., de Ricqlès, A., Horner, J. R. & Padian, K. The evolution and function of thyreophoran dinosaur scutes: implications for plate function in stegosaurs. *Paleobiology* **31**, 291–314 (2005).
- Dubansky, B. H. & Dubansky, B. D. Natural development of dermal ectopic bone in the American alligator (*Alligator mississippiensis*) resembles heterotopic ossification disorders in humans. *Anat. Rec.* **301**, 56–76 (2018).
- Kirby, A. et al. A comparative histological study of the osteoderms in the lizards *Heloderma suspectum* (Squamata: Helodermatidae) and *Varanus komodoensis* (Squamata: Varanidae). *J. Anat.* **236**, 1035–1043 (2020).
- Shadwick, R. E., Russell, A. P. & Lauff, R. F. The structure and mechanical design of rhinoceros dermal armour. *Philos. Trans. R. Soc. Lond. B* **337**, 419–428 (1992).
- Hall, B. K. *Bones and Cartilage, Development and Evolutionary Skeletal Biology* (Elsevier, 2015).
- Galton, P. M. & Upchurch, P. in *The Dinosauria* (eds Weishampel, D. B. et al.) 343–362 (Univ. California Press, 2004).
- Barrett, P. M., Clarke, J. B., Brinkman, D. B., Chapman, S. D. & Ensom, P. C. Morphology, histology and identification of the ‘granicones’ from the Purbeck Limestone Formation (Lower Cretaceous: Berriasian) of Dorset, southern England. *Cretac. Res.* **23**, 279–295 (2002).
- Burns, M. E. & Currie, P. J. External and internal structure of ankylosaur (Dinosauria, Ornithischia) osteoderms and their systematic relevance. *J. Vertebr. Paleontol.* **34**, 835–851 (2014).
- Norman, D. B. *Scelidosaurus harrisonii* (Dinosauria: Ornithischia) from the Early Jurassic of Dorset, England: biology and phylogenetic relationships. *Zoo. J. Linn. Soc.* **191**, 1–86 (2021).
- Scheyer, T. M., Syromyatnikova, E. V. & Danilov, I. G. Turtle shell bone and osteoderm histology of Mesozoic and Cenozoic stem-trionychian Adocidae and Nanhsiungchelyida (Crypodira: Adocusia) from Central Asia, Mongolia and North America. *Foss. Rec.* **20**, 69–85 (2017).
- Cerda, I. A., Desojo, J. B. & Scheyer, T. M. Novel data on aetosaur (Archosauria: Pseudosuchia) osteoderm microanatomy and histology: palaeobiological implications. *Palaeontology* **61**, 721–745 (2018).
- D’Emic, M. D., Wilson, J. A. & Chatterjee, S. The titanosaur (Dinosauria: Sauropoda) osteoderm record: review and first definitive specimen from India. *J. Vertebr. Paleontol.* **29**, 165–177 (2009).
- Scheyer, T. M., Desojo, J. B. & Cerda, I. A. Bone histology of phytosaur, aetosaur, and other archosauriform osteoderms (Eureptilia, Archosauromorpha). *Anat. Rec.* **297**, 240–260 (2014).
- Cerda, I. A., García, R. A., Powell, J. E. & Lopez, O. Morphology, microanatomy and histology of titanosaur (Dinosauria, Sauropoda) osteoderms from the Upper Cretaceous of Patagonia. *J. Vertebr. Paleontol.* **35**, e905791 (2015).
- Stocker, M. R. & Butler, R. J. in *Anatomy, Phylogeny and Palaeobiology of Early Archosaurs and their Kin* (eds Nesbitt, S. J. et al.) 91–117 (Geological Society, London, 2013).
- Desojo, J. B., et al. in *Anatomy, Phylogeny and Palaeobiology of Early Archosaurs and their Kin* (eds Nesbitt, S. J. et al.) 203–239 (Geological Society, London, 2013).
- Gaffney, E. S. The comparative osteology of the Triassic turtle *Proganochelys*. *Bull. Am. Mus. Nat. Hist.* **194**, 1–263 (1990).
- Gorsack, E. & O’Connor, P. M. Time-calibrated models support congruency between Cretaceous continental rifting and titanosaurian evolutionary history. *Biol. Lett.* **12**, 20151047 (2016).
- Maidment, S. C. R. Stegosauria: a historical review of the body fossil record and phylogenetic relationships. *Swiss J. Geosci.* **103**, 199–210 (2010).
- Reichel, M., Schultz, C. L. & Soares, M. B. A new traversodontid cynodont (Therapsida, Eucynodontia) from the Middle Triassic Santa Maria Formation of Rio Grande do Sul, Brazil. *Palaentology* **52**, 229–250 (2009).
- Scheyer, T. M. & Sues, H. D. Expanded dorsal ribs in the Late Triassic pseudosuchian reptile *Euscolosuchus olsenii*. *J. Vertebr. Paleontol.* **37**, e1248768 (2017).

39. Salgado, L. et al. A new primitive neornithischian dinosaur from the Jurassic of Patagonia with gut contents. *Sci. Rep.* **7**, 42778 (2017).
40. Molnar, R. E. & Wiffen, J. A Late Cretaceous polar dinosaur fauna from New Zealand. *Cretac. Res.* **15**, 689–706 (1994).
41. Coria, R. A. & Salgado, L. in *The Armored Dinosaurs* (ed. Carpenter, K.) 159–168 (Indiana Univ. Press, 2001).
42. Nath, T. T., Yadagiri, P. & Moitra, A. K. First record of armoured dinosaur from the Lower Jurassic Kota Formation, Pranhita-Godavari Valley, Andhra Pradesh. *J. Geol. Soc. India* **59**, 575–577 (2002).
43. de Valais, S., Apesteguía, S. & Udrizar Sauthier, D. Neuvas evidencias de dinosaurios de la Formación Puerto Yeruá (Cretácico), Provincia de Entre Ríos, Argentina. *Ameghiniana* **40**, 631–635 (2003).
44. Salgado, L. & Gasparini, Z. Reappraisal of an ankylosaurian dinosaur from the Upper Cretaceous of James Ross Island (Antarctica). *Geodiversitas* **28**, 119–135 (2006).
45. Barrett, P. M. et al. Ankylosaurian dinosaur remains from the Lower Cretaceous of southeastern Australia. *Alcheringa* **34**, 205–217 (2010).
46. Leahy, L. G. & Salisbury, S. W. First evidence of ankylosaurian dinosaurs (Ornithischia: Thyreophora) from the mid-Cretaceous (late Albian–Cenomanian) Winton Formation of Queensland, Australia. *Alcheringa* **37**, 249–257 (2013).
47. Galton, P. M. Earliest record of an ankylosaurian dinosaur (Ornithischia: Thyreophora): dermal armour from the Lower Kota Formation (Lower Jurassic) of India. *Neues Jahrb. Geol. Palaeontol. Abh.* **291**, 205–219 (2019).
48. Carpenter, K., Miles, C. & Cloward, K. Skull of a Jurassic ankylosaur. *Nature* **393**, 782–783 (1998).
49. Kirkland, J. I. & Carpenter, K. North America's first pre-Cretaceous ankylosaur (Dinosauria) from the Upper Jurassic Morrison Formation of western Colorado. *BYU Geol. Stud.* **40**, 25–41 (1994).
50. Carpenter, K., Miles, C. A., & Cloward, K. in *The Armored Dinosaurs* (ed. Carpenter, K.) 55–75 (Indiana Univ. Press, 2001).
51. Galton, P. M. & Carpenter, K. The plated dinosaur *Stegosaurus longispinus* Gilmore, 1914 (Dinosauria: Ornithischia; Upper Jurassic, western USA), type species of *Alcovasaurus* n. gen. *Neues Jahrb. Geol. Palaeont. Abh.* **279**, 185–208 (2016).
52. Mateus, O., Dinis, J. & Cunha, P. P. The Lourinhã Formation: the Upper Jurassic to lowermost Cretaceous of the Lusitanian Basin, Portugal – landscapes where dinosaurs walked. *Ciênc. Terra* **19**, 75–97 (2017).
53. Sander, P. M. Longbone histology of the Tendaguru sauropods: implications for growth and biology. *Paleobiology* **26**, 466–488 (2000).
54. Padian, K. & Lamm, E. *Bone Histology Of Fossil Tetrapods* (Univ. California Press, 2013).
55. Hayashi, S., Carpenter, K. & Suzuki, D. Different growth patterns between the skeleton and osteoderms of *Stegosaurus* (Ornithischia: Thyreophora). *J. Vertebr. Paleontol.* **29**, 123–131 (2009).
56. Stein, M., Hayashi, S. & Sander, P. M. Long bone histology and growth patterns in ankylosaurs: implications for life history and evolution. *PLoS ONE* **8**, e68590 (2013).
57. Waskow, K. & Mateus, O. Dorsal rib histology of dinosaurs and a crocodile from western Portugal: skeletochronological implications on age determination and life history traits. *C. R. Palevol* **16**, 425–439 (2017).

Acknowledgements

C. Hatch (Natural History Museum) prepared thin sections of the specimen; A. Ball (Natural History Museum) took high-resolution photographs of the slides; B. Creisler (Natural History Museum) advised on etymology. T.M.S. acknowledges support from the Swiss National Science Foundation (grant no. 31003A_179401). We thank the members of the London fossil vertebrates journal club for discussion.

Author contributions

S.C.R.M. and P.M.B. devised the study. D.O. examined the stratigraphy. S.J.S., T.M.S. and E.E.B. carried out histological analysis. V.F. carried out XCT scanning and analysis. S.C.R.M., P.M.B., D.O., S.J.S., T.M.S., E.E.B., V.F., Z.J. and T.J.R. interpreted the data and wrote the manuscript.

Competing interests

The authors declare no competing interests.

Additional information

Extended data is available for this paper at <https://doi.org/10.1038/s41559-021-01553-6>.

Supplementary information The online version contains supplementary material available at <https://doi.org/10.1038/s41559-021-01553-6>.

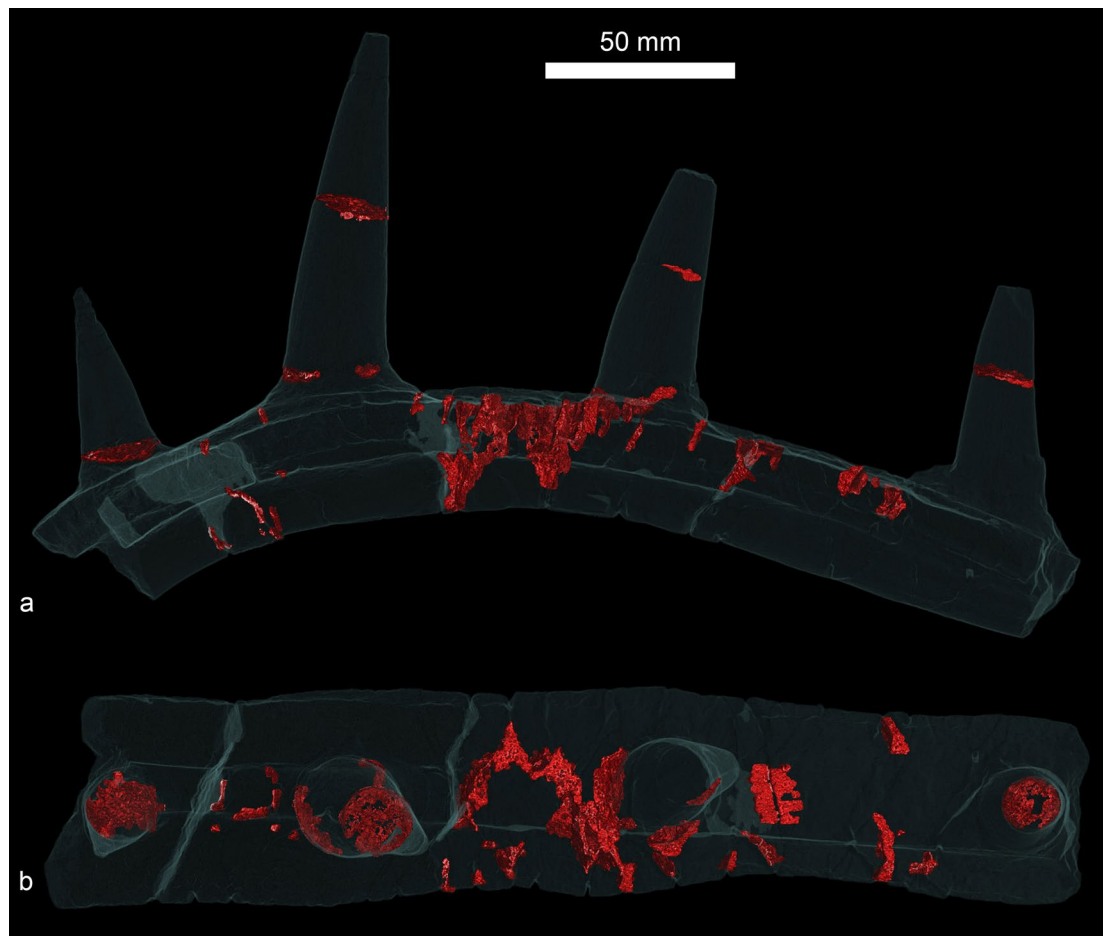
Correspondence and requests for materials should be addressed to Susannah C. R. Maidment.

Peer review information *Nature Ecology & Evolution* thanks the anonymous reviewers for their contribution to the peer review of this work.

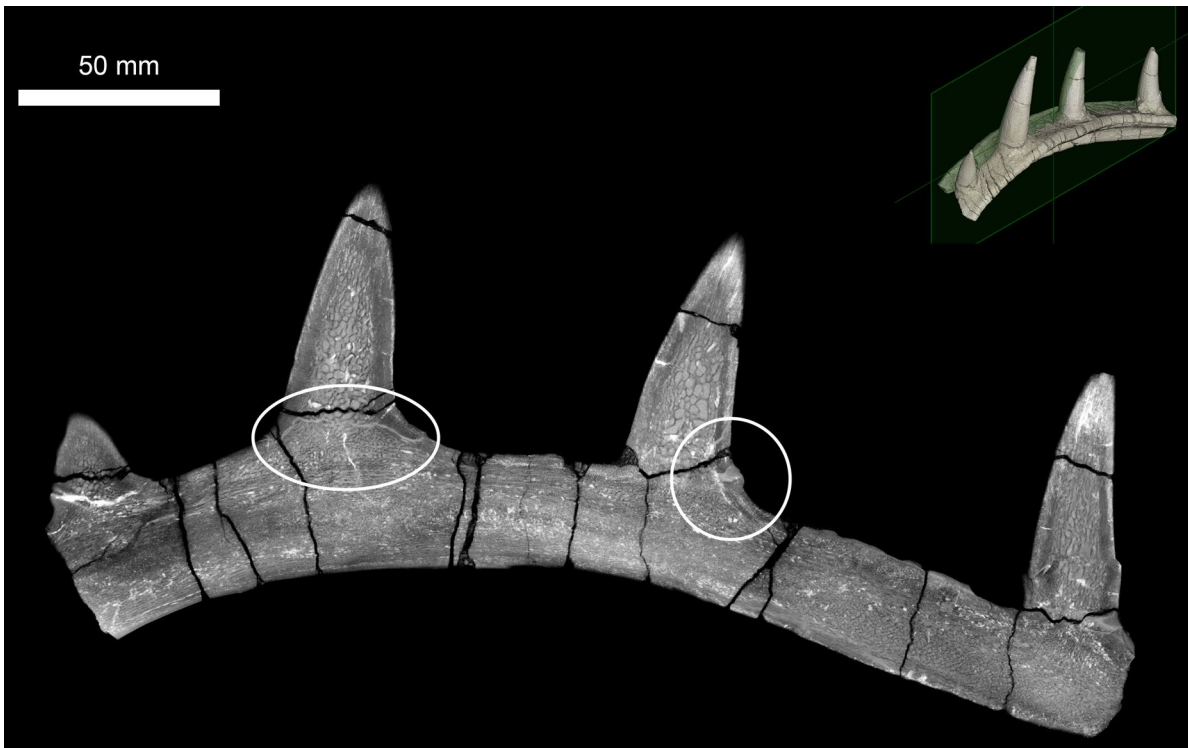
Reprints and permissions information is available at www.nature.com/reprints.

Publisher's note Springer Nature remains neutral with regard to jurisdictional claims in published maps and institutional affiliations.

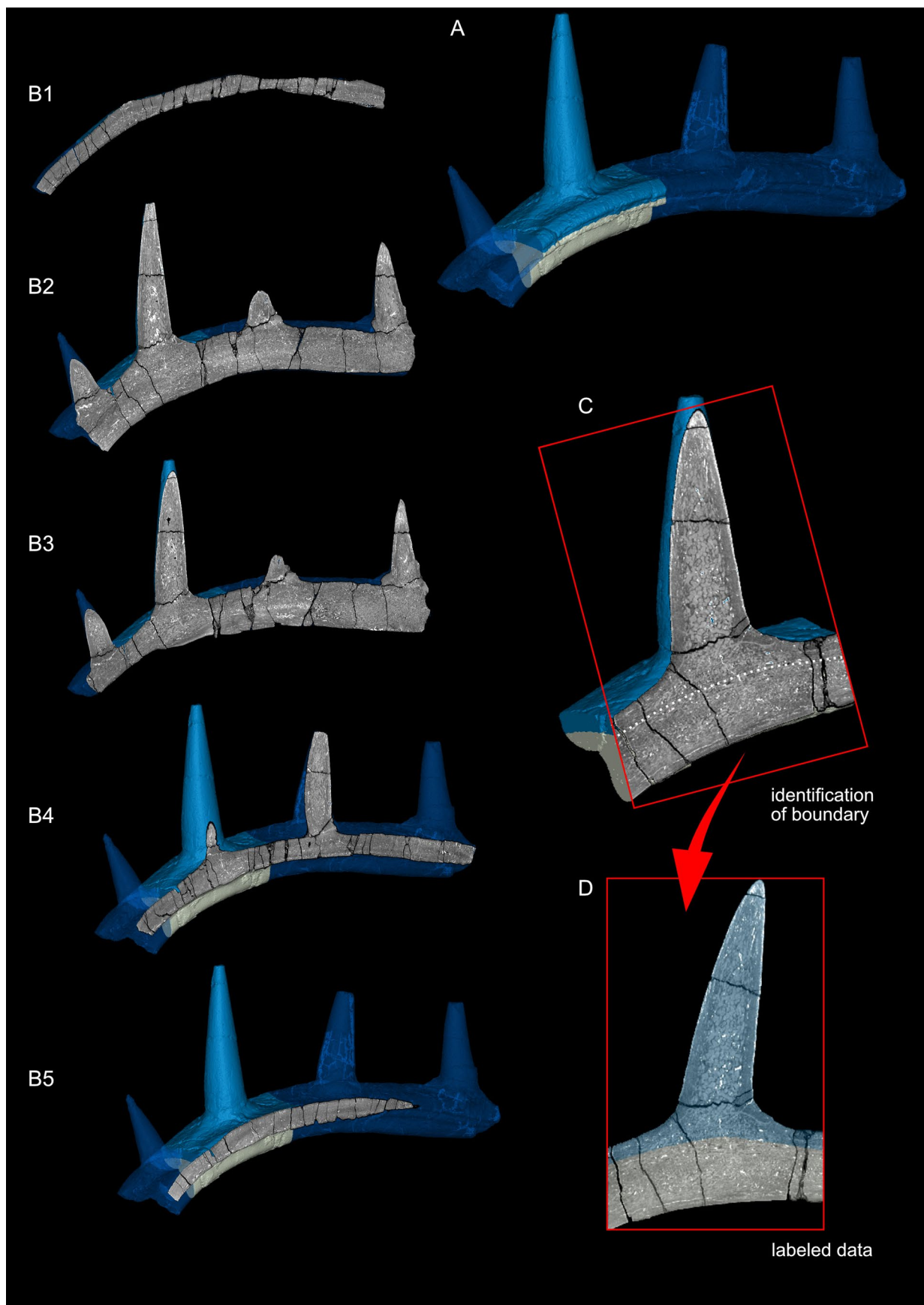
© The Author(s), under exclusive licence to Springer Nature Limited 2021



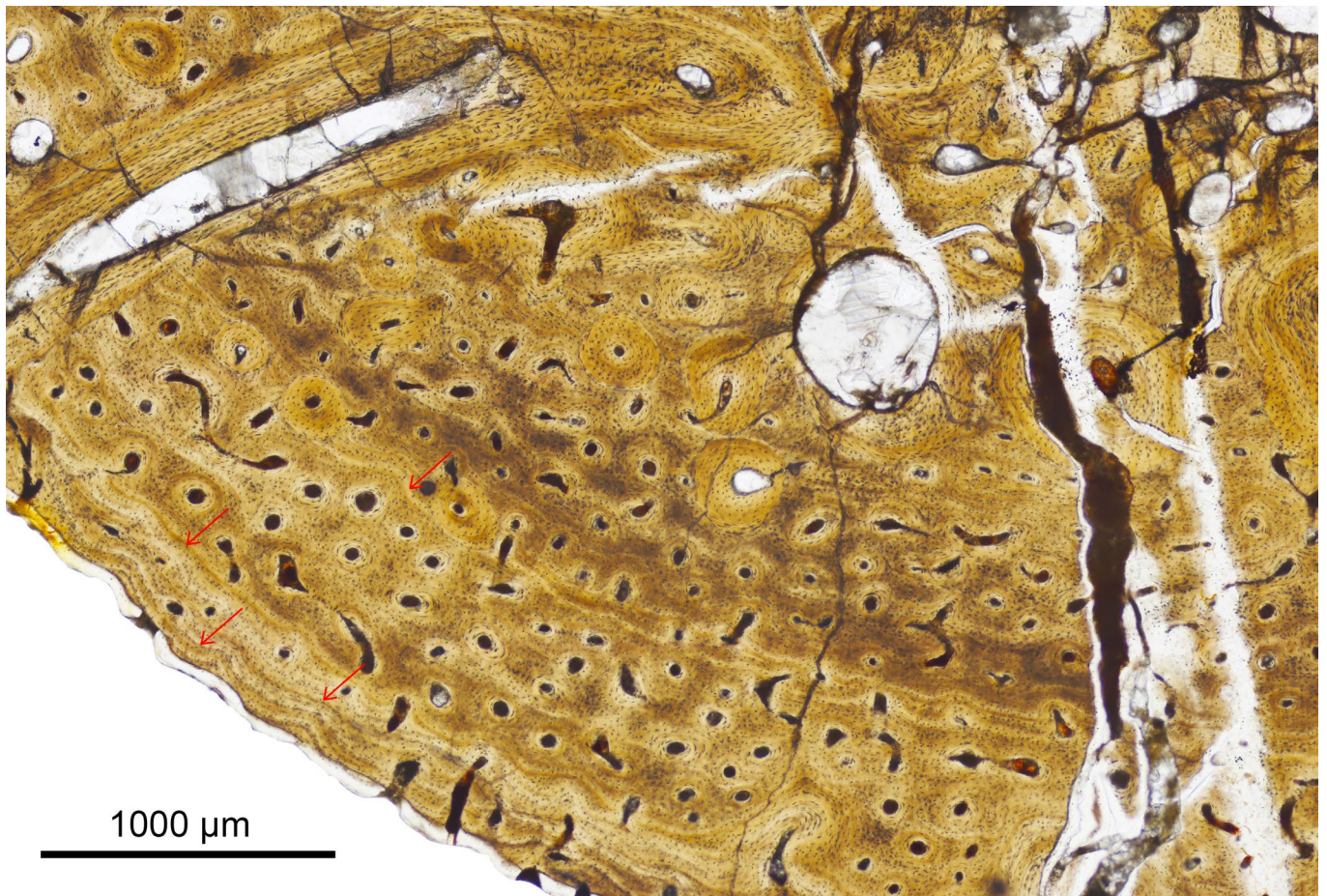
Extended Data Fig. 1 | Translucent XCT reconstruction of NHMUK PV R37412, *Spicomellus afer*. Red shading indicates a grainy cement or fill used to consolidate the specimen. **a**, lateral and **b**, dorsal view. Also see Supplementary video.



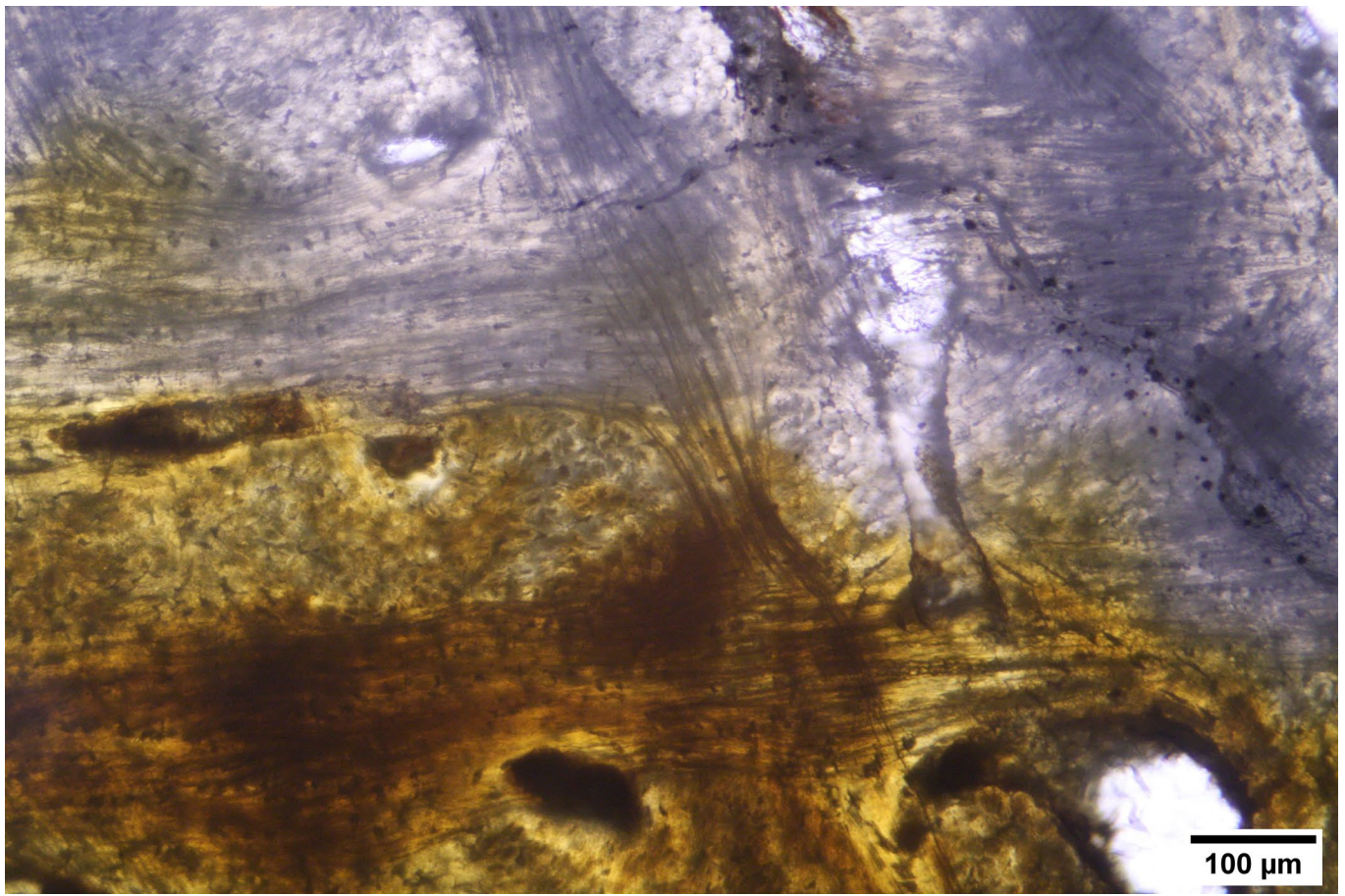
Extended Data Fig. 2 | XCT-scan image of a longitudinal cross-section through NHMUK PV R37412. White ovals highlight areas where it is possible to see the continuity of cortical and trabecular bone from the spikes to the rod.



Extended Data Fig. 3 | The osteoderm and rib parts of the rod were segmented using the following procedure. **a**, a section of the specimen was identified for focus; **b**, longitudinal sections of the specimen were examined in XCT data; **c**, the boundary between the osteoderm and the rib was identified on longitudinal sections; **d**, the data were labelled.



Extended Data Fig. 4 | Histological thin-section (plane polarized light) showing detail of the spine. A vascular channel can be observed in the top left of the image. The woven bone matrix of the cortex is dominated by primary osteons. Scattered secondary osteons can be observed in the mid and inner cortex. Large resorption cavities lined with lamellar bone can be observed in the trabecular bone of the core (top right). Red arrows indicate growth (=resting) lines.



Extended Data Fig. 5 | Thin section photomicrograph (plane-polarized light) showing detail of the structural fibres in the upper osteodermal part of the rod. Structural fibre bundles intersect roughly perpendicular to each other. The opaque cast in the top half of the image is probably diagenetic alteration.

Reporting Summary

Nature Portfolio wishes to improve the reproducibility of the work that we publish. This form provides structure for consistency and transparency in reporting. For further information on Nature Portfolio policies, see our [Editorial Policies](#) and the [Editorial Policy Checklist](#).

Statistics

For all statistical analyses, confirm that the following items are present in the figure legend, table legend, main text, or Methods section.

n/a Confirmed

- The exact sample size (n) for each experimental group/condition, given as a discrete number and unit of measurement
- A statement on whether measurements were taken from distinct samples or whether the same sample was measured repeatedly
- The statistical test(s) used AND whether they are one- or two-sided
Only common tests should be described solely by name; describe more complex techniques in the Methods section.
- A description of all covariates tested
- A description of any assumptions or corrections, such as tests of normality and adjustment for multiple comparisons
- A full description of the statistical parameters including central tendency (e.g. means) or other basic estimates (e.g. regression coefficient) AND variation (e.g. standard deviation) or associated estimates of uncertainty (e.g. confidence intervals)
- For null hypothesis testing, the test statistic (e.g. F , t , r) with confidence intervals, effect sizes, degrees of freedom and P value noted
Give P values as exact values whenever suitable.
- For Bayesian analysis, information on the choice of priors and Markov chain Monte Carlo settings
- For hierarchical and complex designs, identification of the appropriate level for tests and full reporting of outcomes
- Estimates of effect sizes (e.g. Cohen's d , Pearson's r), indicating how they were calculated

Our web collection on [statistics for biologists](#) contains articles on many of the points above.

Software and code

Policy information about [availability of computer code](#)

Data collection No software was used

Data analysis XCT reconstruction was performed using Nikon CT-agent software (Nikon Metrology GmbH, Alzenau, Germany). Reconstruction of the specimen was completed using VG Studio MAX 3.2 (Volume Graphics, Heidelberg, Germany). Macro images of the histological slides were taken using an Axio Imager M2 with an AxioCam HR RS camera. Basic white balance, thresholding, cropping and scaling of images was carried out using FIJI, an ImageJ plugin, Corel PaintShop Pro 19, and Adobe Photoshop.

For manuscripts utilizing custom algorithms or software that are central to the research but not yet described in published literature, software must be made available to editors and reviewers. We strongly encourage code deposition in a community repository (e.g. GitHub). See the Nature Portfolio [guidelines for submitting code & software](#) for further information.

Data

Policy information about [availability of data](#)

All manuscripts must include a [data availability statement](#). This statement should provide the following information, where applicable:

- Accession codes, unique identifiers, or web links for publicly available datasets
- A description of any restrictions on data availability
- For clinical datasets or third party data, please ensure that the statement adheres to our [policy](#)

All data included in this paper is available in the manuscript or in Extended data. The specimen described in this study is deposited in the collections of the Natural History Museum, London, under specimen number NHMUK PV R37412.

Field-specific reporting

Please select the one below that is the best fit for your research. If you are not sure, read the appropriate sections before making your selection.

Life sciences Behavioural & social sciences Ecological, evolutionary & environmental sciences

For a reference copy of the document with all sections, see [nature.com/documents/nr-reporting-summary-flat.pdf](https://www.nature.com/documents/nr-reporting-summary-flat.pdf)

Ecological, evolutionary & environmental sciences study design

All studies must disclose on these points even when the disclosure is negative.

Study description	We describe the osteology and histology of a new dinosaur fossil that we interpret as an ankylosaur, from the Middle Jurassic of the Middle Atlas Mountains, Morocco.
Research sample	A single fossil specimen comprising a dorsal rib with a fused, spiked osteoderm.
Sampling strategy	N/a
Data collection	The specimen was acquired by the Natural History Museum, London, from a commercial fossil dealer based in the UK. The specimen was thin-sectioned using standard palaeohistological techniques at three locations: two cross-sections of a spine and one cross section of the rib and osteoderm.
Timing and spatial scale	N/a
Data exclusions	N/a
Reproducibility	The specimen and thin sections are housed in a public repository in perpetuity and is available for study by other qualified researchers.
Randomization	N/a
Blinding	N/a
Did the study involve field work?	<input type="checkbox"/> Yes <input checked="" type="checkbox"/> No

Reporting for specific materials, systems and methods

We require information from authors about some types of materials, experimental systems and methods used in many studies. Here, indicate whether each material, system or method listed is relevant to your study. If you are not sure if a list item applies to your research, read the appropriate section before selecting a response.

Materials & experimental systems

n/a	Involvement in the study
<input checked="" type="checkbox"/>	<input type="checkbox"/> Antibodies
<input checked="" type="checkbox"/>	<input type="checkbox"/> Eukaryotic cell lines
<input type="checkbox"/>	<input checked="" type="checkbox"/> Palaeontology and archaeology
<input checked="" type="checkbox"/>	<input type="checkbox"/> Animals and other organisms
<input checked="" type="checkbox"/>	<input type="checkbox"/> Human research participants
<input checked="" type="checkbox"/>	<input type="checkbox"/> Clinical data
<input checked="" type="checkbox"/>	<input type="checkbox"/> Dual use research of concern

Methods

n/a	Involvement in the study
<input checked="" type="checkbox"/>	<input type="checkbox"/> ChIP-seq
<input checked="" type="checkbox"/>	<input type="checkbox"/> Flow cytometry
<input checked="" type="checkbox"/>	<input type="checkbox"/> MRI-based neuroimaging

Palaeontology and Archaeology

Specimen provenance	NHMUK PV R37412 was acquired by the Natural History Museum from a commercial fossil dealer, Moussa Direct, based in Cambridge, UK. The locality information was provided by Moussa Direct, and confirmed through discussion with the Moroccan fossil dealer who sold it to Moussa Direct. Work on this specimen was conducted via a Memorandum of Understanding between the Natural History Museum, UK, and the Université Sidi Mohamed Ben Abdellah, Morocco.
Specimen deposition	Natural History Museum, London, UK
Dating methods	N/a
<input type="checkbox"/> Tick this box to confirm that the raw and calibrated dates are available in the paper or in Supplementary Information.	

Ethics oversight

N/a

Note that full information on the approval of the study protocol must also be provided in the manuscript.